

Semi-supervised Multi-feature Learning for Person Re-identification

Dario Figueira[‡], Loris Bazzani[†], Hà Quang Minh[†]

[‡]ISR - Instituto Superior Técnico
Lisboa, Portugal

Marco Cristani[†], Alexandre Bernardino[‡], Vittorio Murino[†]

[†]Pattern Analysis & Computer Vision
Istituto Italiano di Tecnologia
Genova - Italy

Abstract

Person re-identification is probably the open challenge for low-level video surveillance in the presence of a camera network with non-overlapped fields of view. A large number of direct approaches has emerged in the last five years, often proposing novel visual features specifically designed to highlight the most discriminant aspects of people, which are invariant to pose, scale and illumination. On the other hand, learning-based methods are usually based on simpler features, and are trained on pairs of cameras to discriminate between individuals. In this paper, we present a method that joins these two ideas: given an arbitrary state-of-the-art set of features, no matter their number, dimensionality or descriptor, the proposed multi-class learning approach learns how to fuse them, ensuring that the features agree on the classification result. The approach consists of a semi-supervised multi-feature learning strategy, that requires at least a single image per person as training data. To validate our approach, we present results on different datasets, using several heterogeneous features, that set a new level of performance in the person re-identification problem.

1. Introduction

Re-identification is considered one of the fundamental building blocks of any multi-camera automated video-surveillance system. In the presence of a wide-area camera network with non-overlapped fields of view (as in the case of airports, stadiums, train stations, etc.), it allows the association of different instances of the same person across different locations and times.

The most important family of re-identification approaches, to which the proposed approach belongs, is called

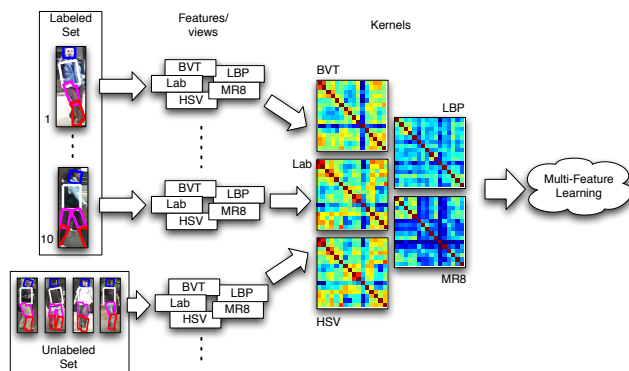


Figure 1. Overview of the proposed method. The features of each individual are extracted from labeled and unlabeled images. Then, kernels are computed for each feature and finally the multi-feature classifier is trained.

appearance-based, since it considers solely the visual aspect of people. Appearance-based methods can be further partitioned in two groups: *direct* and *learning-based*. Direct approaches focus primarily on designing effective descriptors which are invariant to pose, illumination, and scale, by exploiting the morphological aspects of humans and their peculiar characteristics. In particular, body symmetries and textural properties seem to be the most effective cues to distinguish people [7, 8, 12, 11], along with the chromatic distribution. The idea of these approaches is to compute distances among gallery and probe subjects, where a specific similarity measure has to be designed for each cue. The distances are minimized to establish matches among probe and gallery subjects. Multiple features are empirically merged to enrich the signature of a person by a weighted average of the single distances and/or their concatenation (e.g., [11, 19]).

At the other extreme, learning-based methods investigate the aspects which are kept across different fields of view

and which differentiate people the most. Specifically, binary classifiers (*e.g.*, [3, 26]) are usually trained on pairs of instances of the same person (positive class) and pairs of different subjects (negative class). This setup is computationally demanding in real scenarios, because it requires a training set for each pair of cameras, composed by at least two images per person (one for each camera).

In this paper, we propose a learning-based solution that synthesizes the best aspects of both worlds : 1) it allows the exploitation of multiple features independently of their nature and, at the same time 2) it does not require training a classifier for each pair of cameras. Our approach casts re-identification as a semi-supervised multi-class recognition problem, where each class corresponds to the identity of one individual. In particular, we exploit the general framework of multi-view (multi-feature¹ here) learning with manifold regularization in vector-valued Reproducing Kernel Hilbert Spaces (RKHS), recently proposed in [23]. In this setting, each feature is associated with a component of a vector-valued function in an RKHS. Unlike multi-kernel learning [4], all components of a function are forced to map in the same fashion, *i.e.*, to distinguish in a coherent way the different individuals. The desired final output is given by their combination, in a form to be made precise below, which is a fusion mechanism joining together the different features.

As depicted in Fig. 1, the proposed approach trains a classifier from a labeled (gallery) set of P different individuals, exploiting the structure of unlabeled data that can be the probe set or images acquired during tracking. In other words, it does not require to have inter-camera image pairs of the same person, but only a single labeled image per person. This makes our approach truly applicable in real scenarios. In general, unlabeled data can be any acquired image, such as individuals that are not in the gallery set.

The proposed method is compared with several state-of-the-art approaches on several challenging benchmarks. In all of the experiments, we outperform other competing methods, thereby demonstrating the validity of our approach, and encouraging further experiments with novel cues.

The remainder of the paper is organized as follows. In Sec. 2, we briefly review the related literature and our contribution with respect to the state of the art. Sec. 3 fully details our method, along with the features considered in this work. Experiments are then reported in Sec. 4, and, finally, conclusions and future perspectives are given in Sec. 5.

2. Related Work

Following the taxonomy introduced in [11], appearance-based techniques can be divided into *learning-based* and

¹We prefer to use the term multi-feature instead, because views mean different images of the same person in the context of re-identification.

direct methods and into *single-shot* and *multi-shot* approaches.

Learning-based techniques are characterized by the use of a training dataset of different individuals where the features and/or the policy for combining them are analyzed to ensure high re-identification accuracy. The underlying assumption is that the knowledge extracted from the training set generalizes to unseen samples. Binary Support Vector Machines (SVM) [3], multi-class SVM [24], nearest neighbor classifier [20], partial least square reduction [28], boosting [6, 17], distance learning [5, 18, 32], descriptor learning [12], and ensemble RankSVM [26] have been customized for the re-identification problem.

Direct methods do not consider any training sets. These methods are usually focused on finding discriminant parts of the human appearance and manually designing features that perform very well on a particular re-identification scenario. The framed person is typically subdivided into horizontal stripes [13], symmetrical and asymmetrical parts [11], semantic parts [14, 15], regions clustered by color [31], concentric rings [33], or a grid of localized patches [8]. Several features can be extracted from these regions: color histograms or other statistics [13, 11, 15], maximally stable color regions [11], depth features [10], histogram of oriented gradients [28], Gabor and Schmid filters [26], interest points [16], covariance matrices [5, 9], attributes [19] and Haar-like features [6] have been exhaustively tested in the literature.

Single-shot approaches focus on associating pairs of images, each containing one instance of an individual (*e.g.*, [20, 24, 26, 28]). Multi-shot methods employ multiple images of the same person as probe and/or gallery elements (*e.g.*, [8, 11, 14, 29, 27]). The assumption of the multi-shot methods is that individuals are tracked so that it is possible to gather a lot of images. The hope is that the system will obtain a set of images that vary in terms of resolution, partial occlusions, illumination, poses, etc.

Our approach lies in the category of the single-shot learning-based methods. It differs from the related literature for the following reasons: 1) In contrast to all other learning-based strategies, it is able to learn the appearance of the individuals just from one labeled sample and from the additional unlabeled data, *e.g.*, images gathered during tracking. 2) It offers a principled manner to fuse together different modalities/features, enforcing coherence among them.

3. The Proposed Approach

The pipeline of the proposed method is depicted in Fig. 1. The feature descriptors of each individual in the *labeled* and *unlabeled* sets are extracted from detected body parts. Then, the similarity between the descriptors is computed for each feature by mean of kernel matrices (see

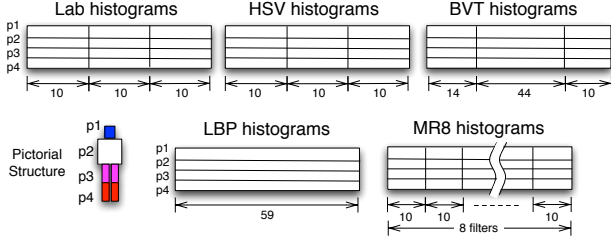


Figure 2. Different features represented by blocks are computed from the detected parts $\{p_i\}_{i=1}^4$.

Sec. 3.1). Multi-feature learning consists in estimating the parameters of the model given the training set (see Sec. 3.2 and Sec. 3.3). Given a probe image, the testing phase consists in computing the similarity of each descriptor with the training samples and use the learned parameter to classify it (see Sec. 3.3).

3.1. Descriptors and Kernels

The first step of the algorithm is to frame the human appearance in order to discard the background information that is considered noise for re-identification. In the same spirit of [14], the pictorial structure (PS) detector [2] is applied to the images of each individual. Then, features are extracted from each of the four parts found by the detector (head, torso, upper-legs and lower-legs, see Fig. 2).

Two complementary aspects of the human appearance often used in the literature for re-identification [11, 12] are extracted from the images: the color distribution and the gradient patterns. For the former, the Black-Value-Tint (BVT) histograms used in [14] and the Hue Saturation Value (HSV) and Lightness color-opponent (Lab) histograms are adopted. For the latter, the Local Binary Pattern (LBP) histograms [25] and the histograms of the Maximum Responses filter banks (MR8) [30] are used. Fig. 2 shows the dimensionality of each feature and how they are concatenated to generate each feature vector.

As described in Sec. 3.3, the learning algorithm requires computing a kernel matrix for each feature. Given the nature of the features, we used the Bhattacharyya kernel to compute similarity between samples, which usually shows good performance when dealing with histograms. Assume that each input vector x can be decomposed into m different views $x = (x^1, \dots, x^m)$ where $x^j \in \mathbb{R}^C$ is the j -th feature descriptor. Then the Bhattacharyya kernel of the i -th feature is defined as follows:

$$k^i(x^i, t^i) = \exp\left(-\frac{D(x^i, t^i)}{(\sigma^i)^2}\right), \quad (1)$$

$$D(x^i, t^i) = \sqrt{1 - \sum_{c=1}^C \sqrt{x_c^i \cdot t_c^i}},$$

where $D(\cdot, \cdot)$ is the Hellinger distance between two distributions (normalized histograms), and σ^i is a parameter estimated as $\sigma^i = \sqrt{2 \cdot D_{\text{med}}^i}$, where D_{med}^i is the median distance of the distance matrix $D(x^i, t^i)$ given each (x^i, t^i) in the training set.

3.2. Multi-feature Learning

The re-identification problem is defined in the multi-feature learning framework of [23], with their *views* corresponding to our *features*, as follows. Suppose that we have access to a training set $\{(x_i, y_i)\}_{i=1}^l \cup \{x_i\}_{i=l+1}^{u+l}$, where $x_i \in \mathcal{X}$ represents the i -th image of the individual with label (identity) $y_i \in \mathcal{Y}$. The first set is called the labeled set with l samples while the second is the unlabeled set with u samples, that is, where y_i is not available. In re-identification, the labeled set corresponds to the gallery set and the unlabeled set can contain either the probe images or arbitrary images gathered during tracking. If the unlabeled set is not available, the method performs supervised learning.

Given that P is the number of identities in the re-identification problem, let the output space be $\mathcal{Y} = \mathbb{R}^P$. Each output label $y_i \in \mathcal{Y}$, $1 \leq i \leq l$, has the form $y_i = (-1, \dots, 1, \dots, -1)$, with 1 at the p -th location if x_i is in the p -th class.

Let the number of features be m . Let $\mathcal{W} = \mathcal{Y}^m = \mathbb{R}^{Pm}$. Let $K : \mathcal{X} \times \mathcal{X} \rightarrow \mathbb{R}^{Pm \times Pm}$ be a matrix-valued positive definite kernel that induces an RKHS \mathcal{H}_K of functions $f : \mathcal{X} \rightarrow \mathcal{W} = \mathbb{R}^{Pm}$. For each function $f \in \mathcal{H}_K$, $f(x) = (f^1(x), \dots, f^m(x))$, where $f^i(x) \in \mathbb{R}^P$ is the value corresponding to the i th feature.

The different features are fused together via a combination operator C as follows

$$Cf(x) = \frac{1}{m}(f^1(x) + \dots + f^m(x)) \in \mathbb{R}^P. \quad (2)$$

In terms of the Kronecker tensor product, C is

$$C = \frac{1}{m} \mathbf{e}_m^T \otimes I_P, \quad (3)$$

where I_P is the $P \times P$ identity matrix and $\mathbf{e}_m = (1, \dots, 1)^T \in \mathbb{R}^m$. Other options to merge the different features may be adopted, but we prefer to not introduce additional parameters that would have to be optimized during training.

Given the training set, re-identification consists of the following optimization problem based on the least square loss function:

$$f^* = \operatorname{argmin}_{f \in \mathcal{H}_K} \frac{1}{l} \sum_{i=1}^l \|y_i - Cf(x_i)\|_2^2 + \gamma_A \|f\|_{\mathcal{H}_K}^2 + \gamma_I \langle \mathbf{f}, M\mathbf{f} \rangle_{\mathcal{W}_{u+l}} \quad (4)$$

with $\mathbf{f} = (f(x_1), \dots, f(x_{u+l}))$ and the regularization parameters $\gamma_A > 0$ and $\gamma_I \geq 0$. The matrix M is defined as $M = I_{u+l} \otimes (M_m \otimes I_P)$, where $M_m = mI_m - \mathbf{e}_m \mathbf{e}_m^T$ [23].

The first term of Eq. 4 is the least square loss function that measures the error between the final output $Cf(x_i)$ for x_i with the given output y_i for each i . The main difference with the standard least square optimization in the first term is that this formulation combines the different features. In particular, if each input instance x has many features, then $f(x) \in \mathcal{W}$ represents the output values from all the features, constructed by their corresponding hypothesis spaces. These values are combined by the operator C to give the final output value in \mathcal{Y} . The second summand is the standard RKHS regularization term. The third summand, multi-feature manifold regularization [23], performs consistency regularization across different features.

3.3. Solution of the Minimization Problem

The solution of the general minimization problem of Eq. 4 is reported in the following². The problem has a unique solution $f^* = \sum_{i=1}^{u+l} K_{x_i} a_i$, where the vectors $a_i \in \mathcal{W}$ are given by the following system of equations:

$$(\mathbf{C}^* \mathbf{C} J_l^{u+l} K[\mathbf{x}] + l\gamma_I M K[\mathbf{x}] + l\gamma_A I) \mathbf{a} = \mathbf{C}^* \mathbf{y}, \quad (5)$$

where $\mathbf{a} = (a_1, \dots, a_{u+l})$ is a column vector in \mathcal{W}^{u+l} and $\mathbf{y} = (y_1, \dots, y_{u+l})$ a column vector in \mathcal{Y}^{u+l} . Here $K[\mathbf{x}]$ denotes the $(u+l) \times (u+l)$ block matrix whose (i, j) block is $K(x_i, x_j)$; J_l^{u+l} is the block diagonal matrix of size $(u+l) \times (u+l)$, with the first l blocks on the main diagonal being $I_{\mathcal{W}}$ and the rest being 0; $\mathbf{C}^* \mathbf{C}$ is the $(u+l) \times (u+l)$ block diagonal matrix, with each diagonal block being $C^* C$; \mathbf{C}^* is the $(u+l) \times (u+l)$ block diagonal matrix, with each diagonal block being C^* .

Assume that each input x is decomposed into $x = (x^1, \dots, x^m)$ for the m different features. Define $K(x, t)$ as a block diagonal matrix, with the (i, i) -th block given by

$$K(x, t)_{i,i} = k^i(x^i, t^i) I_P, \quad (6)$$

where k^i is a kernel of the i -th feature as defined in Sec. 3.1. Define the matrix $G[\mathbf{x}]$ that contains all the kernels as

$$(G(x, t))_{i,i} = k^i(x^i, t^i), \quad (7)$$

and $G[\mathbf{x}]$ as the $(u+l) \times (u+l)$ block matrix, where each block (i, j) is the respective $m \times m$ matrix $G(x_i, x_j)$.

Given this choice of K and $M = I_{u+l} \otimes (M_m \otimes I_P)$, the system of linear equations 5 is equivalent to

$$BA = Y_C, \quad (8)$$

²For the derivations and the proofs of the equations contained in this paper, we refer to the original paper [23].

where

$$B = \left(\frac{1}{m^2} (J_l^{u+l} \otimes \mathbf{e}_m \mathbf{e}_m^T) + l\gamma_I (I_{u+l} \otimes M_m) \right) G[\mathbf{x}] + l\gamma_A I_{(u+l)m},$$

which is of size $(u+l)m \times (u+l)m$, A is the matrix of size $(u+l)m \times P$ such that $\mathbf{a} = \text{vec}(A^T)$, and Y_C is the matrix of size $(u+l)m \times P$ such that $\mathbf{C}^* \mathbf{y} = \text{vec}(Y_C^T)$.

Given the matrices B and Y_C , solving the system of linear equations 8 with respect to A is straightforward. Therefore, the learning method is simple to implement and is very efficient in practice.

Evaluation on a Testing Sample. Once A is thus computed, we need to estimate the labels/identities of the probe images $\mathbf{v} = \{v_1, \dots, v_t\} \in \mathcal{X}$. First, we compute $f^*(v_i)$ for each image, and compose the matrix $\mathbf{f}^*(\mathbf{v}) = (f^*(v_1), \dots, f^*(v_t))^T \in \mathbb{R}^{Pmt}$, with

$$f^*(v_i) = \sum_{j=1}^{u+l} K(v_i, x_j) a_j.$$

Let $K[\mathbf{v}, \mathbf{x}]$ denote the $t \times (u+l)$ block matrix, where block (i, j) is $K(v_i, x_j)$ and similarly, let $G[\mathbf{v}, \mathbf{x}]$ denote the $t \times (u+l)$ block matrix, where block (i, j) is the $m \times m$ matrix $G(v_i, x_j)$. Then

$$\mathbf{f}^*(\mathbf{v}) = K[\mathbf{v}, \mathbf{x}] \mathbf{a} = (G[\mathbf{v}, \mathbf{x}] \otimes I_P) \mathbf{a} = \text{vec}(A^T G[\mathbf{v}, \mathbf{x}]^T).$$

In re-identification, \mathbf{v} contains the unlabeled samples, *i.e.*, $\mathbf{v} = \{x_i\}_{i=l+1}^{u+l}$.

For the i -th image of the p -th individual, $f^*(v_i)$ represents the vector that is as close as possible to $y_i = (-1, \dots, 1, \dots, -1)$, with 1 at the p -th location. The identity of the i -th image is estimated *a-posteriori* by taking the index of the maximum value in the vector $f^*(v_i)$.

4. Experimental Evaluation

The experiments are carried out using public datasets to show that: 1) multi-feature learning increases the performance when adding multiple features, and 2) the proposed method outperforms other state-of-the-art techniques.

Datasets. We used standard challenging datasets for re-identification: iLIDS [33], VIPeR [17] and CAVIAR4REID [14]. iLIDS for re-identification [33] contains 119 people and was built from iLIDS Multiple-Camera Tracking Scenario. The challenges are the presence of occlusions and quite large illumination changes. VIPeR [17] contains two views of 632 pedestrians captured from different viewpoints. CAVIAR4REID [14] contains images of pedestrians extracted from the CAVIAR dataset. It has a total of 72 individuals: 50 with two camera views and 22 with one view. The individuals with one view are not considered in our experiments as in [14].

Table 1. Results on iLIDS (left) and VIPeR (right) datasets, comparing the single-feature and multi-feature learning. Best scores in bold, second best scores in italic.

		iLIDS					VIPeR				
Feature		$r = 1$	$r = 5$	$r = 10$	$r = 20$	nAUC	$r = 1$	$r = 5$	$r = 10$	$r = 20$	nAUC
SFL	LBP	11.60	27.06	38.66	53.44	74.36	1.68	7.56	11.71	20.63	66.93
	MR8	12.19	31.85	44.12	55.71	78.75	2.02	8.13	12.82	22.85	73.46
	Lab	24.87	46.81	54.71	65.63	83.42	11.17	28.51	36.90	48.51	85.68
	HSV	24.37	45.55	55.88	66.13	83.27	17.94	38.42	51.99	66.14	91.61
	BVT	26.89	47.48	56.22	66.64	83.96	16.71	34.71	46.30	58.32	88.73
MFL	LBP+MR8	19.92	38.49	49.16	61.43	81.26	3.39	10.06	17.72	28.23	76.56
	LBP+MR8+Lab	26.72	50.08	<i>60.17</i>	<i>72.94</i>	<i>86.96</i>	10.38	24.87	35.35	47.56	85.48
	LBP+MR8+Lab+HSV	29.50	50.34	58.23	71.43	86.81	18.01	37.44	48.73	62.34	91.89
	LBP+MR8+Lab+HSV+BVT	<i>30.76</i>	<i>50.59</i>	58.74	70.42	86.44	<i>19.59</i>	<i>40.76</i>	<i>52.21</i>	<i>66.11</i>	<i>92.34</i>
MFL opt.	LBP+MR8+Lab+HSV+BVT	31.51	51.18	62.43	74.79	88.40	22.53	44.40	55.92	70.70	93.75

Table 2. Results on iLIDS (top), VIPeR (middle) and CAVIAR4REID datasets (bottom), comparing the proposed method with the state of the art. Best scores in bold, second best scores in italic.

		iLIDS				
		$r = 1$	$r = 5$	$r = 10$	$r = 20$	nAUC
SDALF [11]		28.49	48.21	57.28	68.26	84.99
PS [14]		27.39	52.27	<i>60.92</i>	<i>71.85</i>	<i>87.08</i>
[22]		25.97	43.27	55.97	67.31	83.14
[33]		24.00	43.50	54.00	66.00	—
MFL		<i>30.76</i>	50.59	58.74	70.42	86.44
MFL opt.		31.51	<i>51.18</i>	62.43	74.79	88.40

		VIPeR				
		$r = 1$	$r = 5$	$r = 10$	$r = 20$	nAUC
SDALF [11]		19.87	38.89	49.36	65.72	92.24
PS [14]		<i>21.17</i>	<i>42.66</i>	56.90	72.82	<i>93.51</i>
RDC [32]		15.66	38.42	53.86	70.09	—
[21]+RankSVM [26]		15.73	37.66	51.17	66.27	—
[21]+RDC [32]		16.14	37.72	50.98	65.95	—
MFL		19.59	40.76	52.21	66.11	92.34
MFL opt.		22.53	44.40	<i>55.92</i>	<i>70.70</i>	93.75

		CAVIAR4REID				
		$r = 1$	$r = 5$	$r = 10$	$r = 20$	nAUC
SDALF [11]		6.80	25.00	44.40	65.80	68.65
PS [14]		8.60	30.80	47.80	<i>71.60</i>	72.38
MFL		6.40	<i>31.60</i>	<i>48.20</i>	70.60	<i>72.61</i>
MFL opt.		<i>8.20</i>	35.20	53.20	74.00	74.39

Results. Standard metrics are used to evaluate the performance of the proposed method against the state of the art: the Cumulative Match Curve (CMC) and the normalized Area Under the CMC (nAUC). We pay particular attention to the first ranks of the CMCs, $r = \{1, 5, 10, 20\}$, because they better reveal the behavior of the methods in practice. The experiment protocol is consistent with the methods we compare with. Each dataset was randomly split 10 times in gallery and probe sets, and the results shows the average of the results over the different trials. In our experiments, the probe set is considered as unlabeled data.

We first tested the proposed re-identification method in a Single-Feature Learning setup (SFL in Table 1), *i.e.* the kernel of a single feature is used. Then, we added one feature for each experiment to evaluate the increment in performance when including more features, that is the Multi-Feature Learning (MFL) in Table 1. For these experi-

ments, the regularization parameters are empirically set to $\gamma_I = 10^{-5}$ and $\gamma_A = 0.1$ and the kernel parameters (σ^i) were estimated as noted in Sec. 3.1. In the last experiment (MFL opt. in Table 1), the regularization parameters along with the kernel parameters in Eq. 1 were optimized using the pattern search algorithm [1].

The results reported in Table 1 show the results on different datasets: iLIDS on the left and VIPeR on the right. It is easy to notice that MFL is always better than the respective single-feature experiment even when considering just two features. In fact, LBP+MR8 (sixth row) outperforms the SFL experiments of both LBP (first row) and MR8 (second row). The results show also that adding more features increases the accuracy. For the VIPeR dataset, the nAUC increase by 15.78 percentage points from the 2-feature to the 5-feature experiment. The best results are obtained when the parameters are optimized (MFL opt.).

Having demonstrated that the proposed MFL method is able to fuse different features, we now report the results comparing it to the state-of-the-art learning-based and direct techniques proposed in last few years on different datasets. We show in Table 2 the results related to other re-identification techniques. MFL opt. outperforms all the methods in terms of nAUC and almost all the reported points of the CMC. PS is slightly better than MFL opt. in few points: $r = \{10, 20\}$ in VIPeR and $r = 1$ in CAVIAR4REID. In general, MFL opt. outperforms PS when considering the overall statistics on the CMC, such as the nAUC.

5. Conclusions

In this work, a semi-supervised multi-feature learning framework has been proposed to deal jointly with the appearance-based and learning-based re-identification problem. Our solution poses re-identification as a multi-class recognition problem in a single-shot learning setup. An advantage of the presented technique is that it relies on a multi-feature learning framework to properly fuse different modalities and exploits the unlabeled data that are available during tracking. The proposed method opens many

other interesting challenges, such as how to perform on-line learning to include new classes (individuals). Another point that should be investigated is a more complex loss function that considers the structure of the data and the correlation and differences across different classes.

Acknowledgments

This work was partially supported by FCT [PEst-OE/EEI/LA0009/2013] and by the project High Definition Analytics (HDA), QREN - ID in Co-Promocão 13750, and by the project MAIS-S, CMU-PT / SIA / 0023 / 2009 under the Carnegie Mellon-Portugal Program. The work of Dario Figueira was partially supported with grant SFRH/BD/48526/2008, from Fundação para a Ciência e a Tecnologia.

References

- [1] M. A. Abramson. *Pattern search algorithms for mixed variable general constrained optimization problems*. PhD thesis, École Polytechnique de Montréal, 2002.
- [2] M. Andriluka, S. Roth, and B. Schiele. Pictorial structures revisited: People detection and articulated pose estimation. In *CVPR*, 2009.
- [3] T. Avraham, I. Gurvich, M. Lindenbaum, and S. Markovitch. Learning implicit transfer for person re-identification. In *ECCV Workshops*, 2012.
- [4] F. R. Bach, G. R. G. Lanckriet, and M. I. Jordan. Multiple kernel learning, conic duality, and the SMO algorithm. In *ICML*, 2004.
- [5] S. Bak, G. Charpiat, E. Corvee, F. Bremond, and M. Thonnat. Learning to match appearances by correlations in a covariance metric space. In *ECCV*, 2012.
- [6] S. Bak, E. Corvee, F. Bremond, and M. Thonnat. Person Re-identification Using Haar-based and DCD-based Signature. In *AMMCSS*, 2010.
- [7] S. Bak, E. Corvee, F. Bremond, and M. Thonnat. Person Re-identification Using Spatial Covariance Regions of Human Body Parts. In *AVSS*, 2010.
- [8] S. Bak, E. Corvee, F. Bremond, and M. Thonnat. Multiple-shot human re-identification by mean riemannian covariance grid. In *AVSS*, 2011.
- [9] S. Bak, E. Corvee, F. Bremond, and M. Thonnat. Boosted human re-identification using riemannian manifolds. *Image Vision Comput.*, 30(6-7):443–452, June 2012.
- [10] I. B. Barbosa, M. Cristani, A. Bue, L. Bazzani, and V. Murino. Re-identification with rgb-d sensors. In *ECCV*, 2012.
- [11] L. Bazzani, M. Cristani, and V. Murino. Symmetry-driven accumulation of local features for human characterization and re-identification. *Computer Vision and Image Understanding*, 117(2):130 – 144, 2013.
- [12] L. Bazzani, M. Cristani, A. Perina, and V. Murino. Multiple-shot person re-identification by chromatic and epitomic analyses. *Pattern Recognition Letters*, 2011.
- [13] N. Bird, O. Masoud, N. Papanikolopoulos, and A. Isaacs. Detection of loitering individuals in public transportation areas. *IEEE Trans. on Intelligent Transportation Systems*, 6(2):167 – 177, 2005.
- [14] D. S. Cheng, M. Cristani, M. Stoppa, L. Bazzani, and V. Murino. Custom pictorial structures for re-identification. In *BMVC*, 2011.
- [15] D. Figueira and A. Bernardino. Re-Identification of Visual Targets in Camera Networks a comparison of techniques. In *ICIAR*, 2011.
- [16] N. Gheissari, T. B. Sebastian, P. H. Tu, J. Rittscher, and R. Hartley. Person reidentification using spatiotemporal appearance. In *CVPR*, 2006.
- [17] D. Gray and H. Tao. Viewpoint invariant pedestrian recognition with an ensemble of localized features. In *ECCV*, 2008.
- [18] M. Kostinger, M. Hirzer, P. Wohlhart, P. Roth, and H. Bischof. Large scale metric learning from equivalence constraints. In *CVPR*, 2012.
- [19] R. Layne, T. Hospedales, and S. Gong. Person re-identification by attributes. In *BMVC*, 2012.
- [20] Z. Lin and L. S. Davis. Learning pairwise dissimilarity profiles for appearance recognition in visual surveillance. In *Advances in Visual Computing*, 2008.
- [21] C. Liu, S. Gong, C. Loy, and X. Lin. Person re-identification: What features are important? In *ECCV Workshops*. 2012.
- [22] N. Martinel and C. Micheloni. Re-identify people in wide area camera network. In *CVPR Workshops*, 2012.
- [23] H. Q. Minh, L. Bazzani, and V. Murino. A unifying framework for vector-valued manifold regularization and multi-view learning. In *ICML*, volume 28, pages 100–108, 2013.
- [24] C. Nakajima, M. Pontil, B. Heisele, and T. Poggio. Full-body person recognition system. *Pattern Recognition Letters*, 36(9):1997–2006, 2003.
- [25] T. Ojala, M. Pietikainen, and T. Maenpaa. Multiresolution gray-scale and rotation invariant texture classification with local binary patterns. *IEEE Trans. Pattern Anal. Mach. Intell.*, 24(7):971–987, 2002.
- [26] B. Prosser, W. Zheng, S. Gong, and T. Xiang. Person re-identification by support vector ranking. In *BMVC*, 2010.
- [27] P. Salvagnini, L. Bazzani, M. Cristani, and V. Murino. Person re-identification with a ptz camera: an introductory study. In *ICIP*, 2013.
- [28] W. R. Schwartz and L. S. Davis. Learning discriminative appearance-based models using partial least squares. In *Proceedings of the XXII Brazilian Symposium on Computer Graphics and Image Processing*, 2009.
- [29] J. Sivic, C. L. Zitnick, and R. Szeliski. Finding people in repeated shots of the same scene. In *BMVC*, 2006.
- [30] M. Varma and A. Zisserman. A statistical approach to texture classification from single images. *IJCV*, 2005.
- [31] X. Wang, G. Doretto, T. B. Sebastian, J. Rittscher, and P. H. Tu. Shape and appearance context modeling. In *ICCV*, 2007.
- [32] W. Zheng, S. Gong, and T. Xiang. Re-identification by relative distance comparison. *IEEE Trans. Pattern Anal. Mach. Intell.*, PP(99):1, 2012.
- [33] W. S. Zheng, S. Gong, and T. Xiang. Associating groups of people. In *BMVC*, 2009.